2013

Ventilation rates and activity levels of juvenile jumbo squid under metabolic suppression in the oxygen minimum zone

Katja Trübenbach

Maria R. Pegado

Brad A. Seibel
University of Rhode Island, seibel@usf.edu

Rui Rosa

Citation/Publisher Attribution
Trübenbach, K., Pegado, M. R., Seibel, B. A., & Rosa, R. (2013). Ventilation rates and activity levels of juvenile jumbo squid under metabolic suppression in the oxygen minimum zone. *Journal of Experimental Biology, 216*, 359-368. doi: 10.1242/jeb.072587
Available at: http://dx.doi.org/10.1242/jeb.072587

The Journal of Experimental Biology 216, 359-368

doi:10.1242/jeb.072587

RESEARCH ARTICLE

Ventilation rates and activity levels of juvenile jumbo squid under metabolic suppression in the oxygen minimum zone

Katja Trübenbach[1,*], Maria R. Pegado[1], Brad A. Seibel[2] and Rui Rosa[1]

[1]Laboratório Marítimo da Guia, Centro de Oceanografia, Faculdade de Ciências da Universidade de Lisboa, Av. Nossa Senhora do Cabo, 939, 2750-374 Cascais, Portugal and [2]Center for Biotechnology and Life Sciences, Biological Sciences, University of Rhode Island, 120 Flagg Road, Kingston, RI 02881, USA

*Author for correspondence (kjtrubenbach@fc.ul.pt)

SUMMARY

The Humboldt (jumbo) squid, *Dosidicus gigas*, is a part-time resident of the permanent oxygen minimum zone (OMZ) in the Eastern Tropical Pacific and, thereby, it encounters oxygen levels below its critical oxygen partial pressure. To better understand the ventilatory mechanisms that accompany the process of metabolic suppression in these top oceanic predators, we exposed juvenile *D. gigas* to the oxygen levels found in the OMZ (1% O_2, 1 kPa, 10°C) and measured metabolic rate, activity cycling patterns, swimming mode, escape jet (burst) frequency, mantle contraction frequency and strength, stroke volume and oxygen extraction efficiency. In normoxia, metabolic rate varied between 14 and 29 μmol O_2 g^{-1} wet mass h^{-1}, depending on the level of activity. The mantle contraction frequency and strength were linearly correlated and increased significantly with activity level. Additionally, an increase in stroke volume and ventilatory volume per minute was observed, followed by a mantle hyperinflation process during high activity periods. Squid metabolic rate dropped more than 75% during exposure to hypoxia. Maximum metabolic rate was not achieved under such conditions and the metabolic scope was significantly decreased. Hypoxia changed the relationship between mantle contraction strength and frequency from linear to polynomial with increasing activity, indicating that, under hypoxic conditions, the jumbo squid primarily increases the strength of mantle contraction and does not regulate its frequency. Under hypoxia, jumbo squid also showed a larger inflation period (reduced contraction frequency) and decreased relaxed mantle diameter (shortened diffusion pathway), which optimize oxygen extraction efficiency (up to 82%/34%, without/with consideration of 60% potential skin respiration). Additionally, they breathe 'deeply', with more powerful contractions and enhanced stroke volume. This deep-breathing behavior allows them to display a stable ventilatory volume per minute, and explains the maintenance of the squid's cycling activity under such O_2 conditions. During hypoxia, the respiratory cycles were shorter in length but increased in frequency. This was accompanied by an increase in the number of escape jets during active periods and a faster switch between swimming modes. In late hypoxia (onset ~170±10 min), all the ventilatory processes were significantly reduced and followed by a lethargic state, a behavior that seems closely associated with the process of metabolic suppression and enables the squid to extend its residence time in the OMZ.

Supplementary material available online at http://jeb.biologists.org/cgi/content/full/216/3/359/DC1

Key words: hypoxia, OMZ, jet propulsion, ventilation, jumbo squid, *Dosidicus gigas*, metabolic suppression.

Received 13 March 2012: Accepted 7 September 2012

INTRODUCTION

Dosidicus gigas (jumbo or Humboldt squid) is the largest ommastrephid squid (up to 2.5 m length and 50 kg in mass) (Nesis, 1983) and has one the highest metabolic rates of any animal in the ocean (Rosa and Seibel, 2008). It is endemic to the Eastern Pacific, and particularly abundant in the highly productive waters of the California and Peru Current systems (Nigmatullin et al., 2001) and the Costa Rica Dome (Ichii et al., 2002; Waluda and Rodhouse, 2006), where it plays a crucial role both as prey (Clarke and Paliza, 2001; Abitía-Cárdenas et al., 2002; Ruiz-Cooley et al., 2004) and predator (Markaida and Sosa-Nishizaki, 2003). In addition to its ecological role, the Humboldt squid is an economically important species and the target of the world's largest cephalopod fishing industry (Rodhouse et al., 2006).

In addition to seasonal horizontal migrations (Markaida et al., 2005), *D. gigas* undergoes diel vertical migrations into mesopelagic depths (around 250 m) during the daytime (Gilly et al., 2006) (Trueblood and Seibel, 2012), similar to the migration pattern of their primary prey – myctophid fishes (Markaida and Sosa-Nishizaki, 2003; Markaida et al., 2008). While at depth, *D. gigas* encounters the permanent oxygen minimum zone (OMZ) of the Eastern Tropical Pacific during the day, with oxygen levels often less than 5 μmol l^{-1} (~0.5% O_2) (Kamykowski and Zentara, 1990; Morrison et al., 1999). Other top pelagic predators (e.g. tuna, swordfish, marlin and sharks) (Brill, 1994; Prince and Goodyear, 2006; Vetter et al., 2008; Nasby-Lucas et al., 2009; Stramma et al., 2012) seem to avoid these hypoxic depths, as their tolerance to hypoxic conditions is low [<150 μmol l^{-1} O_2 (Brill, 1994; Brill, 1996); ~45 μmol l^{-1} O_2, big-eye tuna (Lowe et al., 2000)]. One might expect that the presence of active, muscular squid in these hypoxic zones would be precluded, as, in other active squid: (i) the primary mode of locomotion, jet propulsion, is energetically inefficient (Webber et al., 2000); (ii) the oxygen-carrying capacity is limitative relative to that of fishes, requiring that cephalopods use most of the O_2 in the blood on each

cycle, leaving little venous oxygen reserve behind (Pörtner, 2002); (iii) the oxygen-carrying capacity is low because of viscosity-related constraints and an extracellular low-affinity respiratory protein (Pörtner, 2002); and (iv) ventilatory and locomotory systems are closely tied. Regarding the last of these, two different strategies evolved in these mollusks to deal with this restriction. Pelagic squid (like *D. gigas*) that routinely depend on jet propulsion optimize their locomotory apparatus by pushing a large water volume through their mantle cavity, reducing oxygen extraction efficiency (5–10%) (Pörtner, 1994; Wells et al., 1988). In contrast, nekton-benthic cephalopods (i.e. cuttlefish and octopus) developed an efficient oxygen uptake system (40–50%) (Wells and Wells, 1985) by minimizing their ventilatory volume to increase diffusion (Wells et al., 1988).

Squid are thought to live chronically 'on the edge of oxygen limitation' (Pörtner, 2002) and are not well poised to adapt to low ambient O_2 levels. Yet, the Humboldt squid has managed to minimize the trade-offs between high locomotory performance and hypoxia tolerance *via* metabolic suppression (Rosa and Seibel, 2008; Rosa and Seibel, 2010), coupled with a high-affinity respiratory protein (Seibel, 2012). Here, we exposed juvenile squid to oxygen levels found in the OMZ (1% O_2, 1 kPa, 10°C, severe hypoxia) to investigate the effects on the ventilatory mechanisms that accompany the process of metabolic suppression in *D. gigas*, namely: (i) maximal, active, routine and inactive metabolic rates; (ii) metabolic scope; (iii) activity cycling patterns and swimming mode (with video recording); (iv) escape jet (burst) frequency; (v) mantle contraction frequency and strength; (vi) stroke volume, and ventilatory volume per minute; and (vii) oxygen extraction efficiency (with and without a potential contribution from skin respiration).

MATERIALS AND METHODS

Specimen collection

Juvenile Humboldt squid, *D. gigas* (d'Orbigny 1835), (5.4–13.5 g wet mass) were collected *via* dip net in the Gulf of California (27°N, 111°W; 28°N, 113°W), on the surface at night, in June 2011 (aboard the RV *New Horizon*, Scripps Institute, CA, USA) and were immediately transferred to aquaria containing 10°C seawater (environmental temperature at OMZ) on board the vessel. It is worth noting that all experiments were conducted with juvenile stages, and it is not known whether juvenile and adult jumbo squid display similar diel vertical migration behavior (i.e. whether they encounter the same minimum oxygen levels during descent).

Experimental procedure

Animals were placed in a flow-through respirometry set up (270 ml volume, Loligo Systems, Tjele, Denmark) (Rosa and Seibel, 2008; Rosa and Seibel, 2010), and allowed to acclimate for 8–12 h before measurements of oxygen consumption were started. Respirometers were immersed in a large thermostatically controlled waterbath (Lauda, Lauda-Königshofen, Germany) at 10°C, a temperature approximating that found at 250 m in the OMZ (Rosa and Seibel, 2010). Filtered (0.2 μm) and treated (50 mg l^{-1} streptomycin) seawater was pumped from a water-jacketed, gas-equilibration column through the respirometers at a constant flow rate (average 120 ml min^{-1}). The water in the column was bubbled continuously to maintain incoming water at high (21% O_2, 21 kPa,) or low P_{O_2} (certified gas mixture with 1% O_2, 1 kPa). Once the final 1% O_2 level in the respiration chambers had been reached, the first 30 min were excluded, as they may represent an acclimatory phase after adjusting to a new oxygen concentration. Oxygen concentrations were recorded at the entrance and the exit of each chamber with two Clarke-type O_2 electrodes connected to a 928 Oxygen Interface (Strathkelvin Instruments, North Lanarkshire, UK). The system was calibrated using air- and nitrogen-saturated seawater and checked for electrode drift and for microbial oxygen consumption before and after each trial. All experiments were carried out in darkness and at atmospheric pressure. Video recordings were conducted (Sony DCR-SR78, Lisbon, Portugal) during respiration runs. Afterwards, specimens were immediately weighed on a motion-compensated precision shipboard balance system (Childress and Mickel, 1980). A total of 18 specimens were investigated, with 6 replicates for the normoxic treatment (21% O_2, 21 kPa) and 12 for the hypoxic one (1% O_2, 1 kPa). Because of differences in squid swimming behavior (i.e. mantle contraction frequency per minute) and respiratory profile pattern (i.e. number of cycles) throughout hypoxia, this treatment was subdivided into early hypoxia (EH, hypoxia exposure time 30–160 min, N=6) and late hypoxia (LH, hypoxia exposure time >180 min, N=6). Exposure times are presented in Table 1.

Swimming behavior, metabolic rate and cycling performance

Swimming behavior

Jet propulsion was subdivided into three swimming modes, based on previous studies (Gosline et al., 1983; Bartol, 2001); namely: (1) respiratory movements, (2) steady jetting and (3) bursts/escape jets *via* video footage. Respiratory movements were defined by weak mantle contractions without visible thrust. Thereby, squid could be within the water column or, under LH, even lie at the bottom of the chambers. Steady jetting ranged from slow cruising (weak but visible thrusts) to vigorous jetting (powerful thrusts). Bursts or escape jets were characterized by hyperinflation (≥5% increase of relaxed mantle diameter) followed by maximum mantle contraction (Gosline and DeMont, 1985) and fast movements. The relaxed diameter was assessed under normoxia at inactive metabolic rate (IMR) using ImageJ software (Wayne Rasband, National Institute of Mental Health, Bethesda, MD, USA), as mantle contractions at slow swimming speeds occur without hyperinflation (Gosline and DeMont, 1985). The number of escape jets per minute was quantified *via* video analysis.

Metabolic rate

The number of escape jets per minute and the swimming modes were linked to changes in O_2 consumption during cycling periods. Based on this, inactive, routine, active and maximum active metabolic rate (IMR, RMR, AMR and MR_{max}, respectively) could be distinguished (see Table 2, Fig. 1) with similar results to those of a previous study (Rosa and Seibel, 2008). RMR for normoxia and hypoxia was specified as the average rate for the entirety of

Table 1. Exposure times of *Dosidicus gigas* to normoxic (21% O_2) and hypoxic (1% O_2) conditions

	Exposure time (min)		Onset of late hypoxia (min)
N	Normoxia	Hypoxia	
1	662	199	153
2	762	190	164
3	263	189	182
4	263	202	183
5	560	198	163
6	881	188	153
Mean	582	194	166
s.d.	268	6	13

Values are presented individually and as means and standard deviations. Exposure times for hypoxia include acclimation time (30 min).

Table 2. Different activity levels in *Dosidicus gigas*

	MR_{max}	AMR	RMR	IMR
% RMR	≥35	≥15 to <35		≥ –15
Swimming mode	2–3	1–3	1–3	1 (≥75%)
Burst frequency (bursts min^{-1})	≥4	≥4	<4	<4

Activity levels were defined as inactive, routine, active and maximum active metabolic rate (IMR, RMR, AMR and MR_{max}) and are given in terms of burst frequency (bursts min^{-1}) and swimming behavior (mode and % of time for IMR), resulting in percentage classes of oxygen consumption rate based on RMR (see Rosa and Seibel, 2008). Note that RMRs were specified separately for normoxic and hypoxic conditions and quantified as the average of the entire recording. Swimming modes were classified based on previous criteria (Gosline et al., 1983; Bartol, 2001): 1, respiratory movement; 2, steady jetting; and 3, burst/escape jetting.

each recording. During periods of activity, metabolic rate was ≥15–35% (AMR) and >35–100% (MR_{max}) higher than the routine levels (RMR) with escape jets ≥4 bursts min^{-1}. Thus, the AMR and MR_{max} were quantified by averaging the metabolic rates for all peaks exceeding ≥15% or >35%, respectively. Inactive metabolic rate was defined *via* swimming mode 1 (≥75% of time) and burst events <<4 min^{-1}. These periods of apparent inactivity in the chambers correlated with metabolic rates ≤15% lower than RMR and average rates were calculated. Note that pelagic predators such as *D. gigas* rarely stop swimming in nature and that we did not quantify locomotion continuously for all experiments in its entirety. However, our IMR calculations seem to be a reasonable approximation to the criteria set for standard metabolic rate in mammals and other model organisms. Metabolic rate was quantified as μmol O_2 g^{-1} wet mass h^{-1}. The metabolic scope was calculated as the difference between maximum and minimum O_2 consumption.

Cycling performance

All control (normoxia) animals and the majority in early hypoxia (5 out of 6) animals showed a distinct periodicity in their rate of oxygen consumption (Fig. 1). These respiratory cycles are characterized by a steep increase in metabolic rate (~first 1/3 of total cycle length, Fig. 1) and video analysis confirmed that this was linked to an elevation in mantle contraction frequency. The remaining cycle length (Fig. 1) consisted of a slow transition from powerful to weaker mantle contractions. Therefore, burst frequency (number of escape jets per minute, calculated over the entire cycle length) and swimming modes were used to describe those respiratory cycles. Periodicity was further investigated by assessing the number of active and maximum active cycles per hour, including their length in minutes (*via* respiratory files).

Mantle contraction frequency and strength

In cephalopods, locomotion and respiration are closely tied and therefore counterproductive in their goals, even though in resting *Sepia* and probably to some extent in squid, ventilatory and locomotory mechanisms can be uncoupled *via* a collar flap system (Bone et al., 1994). However, both ventilatory and locomotory systems are highly dependent on the frequency and strength of mantle contractions, which, in turn, influence the water volume throughput. Mantle contraction frequency (ventilation rate) was quantified as the number of mantle contractions per minute

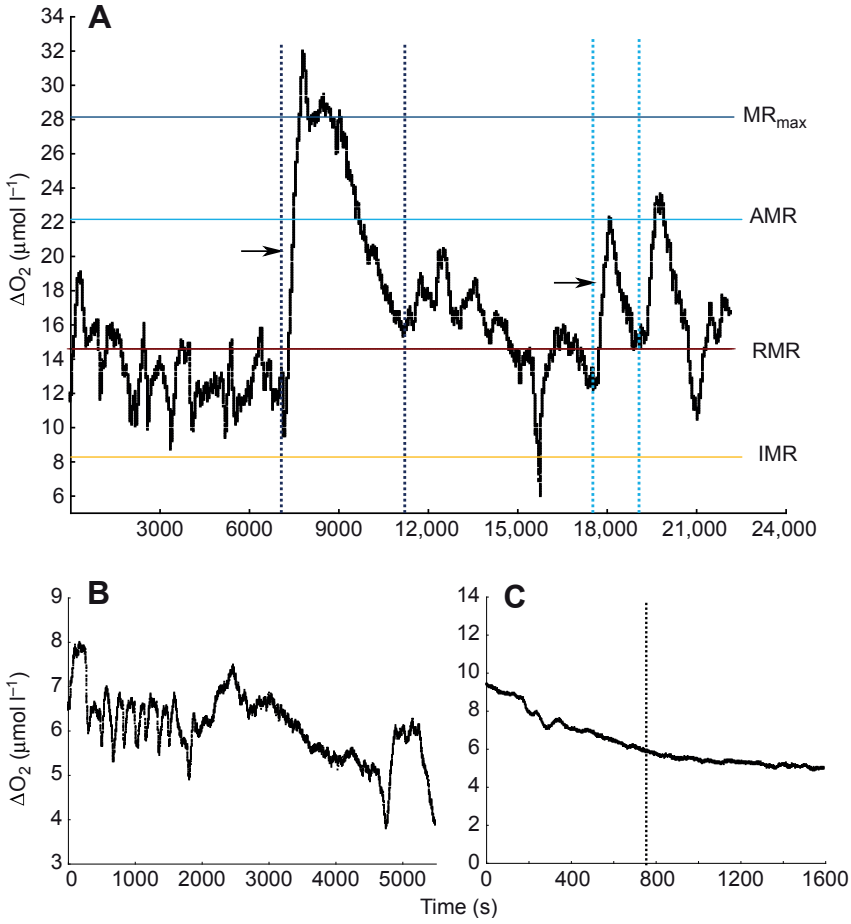

Fig. 1. Oscillations in oxygen levels (ΔO_2) that reflect differences between the values recorded at the entrance and the exit of the chamber in normoxia (A, 10.9 g squid), early hypoxia (B, 1% O_2, 5.4 g squid) and late hypoxia (C, 11.6 g squid) at 10°C. Solid lines in A represent the thresholds for inactive (IMR), routine (RMR), active (AMR) and maximum metabolic rate (MR_{max}) (illustrated in Table 2). Black arrows indicate the acceleration phase of MR_{max} and AMR cycles, and the vertical dashed lines mark the respective cycle lengths. The dashed line in C represents the onset of late hypoxia (170±10 min, *N*=6). Note, the 0 value on the *x*-axis in the hypoxia plots (B,C) does not represent the real onset of hypoxia.

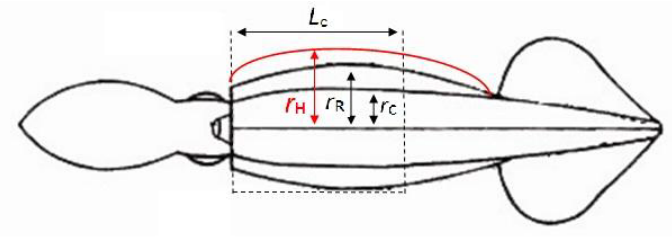

Fig. 2. Schematic drawing of a squid with descriptions of the measurements used to quantify ventilation stroke volume and hyperinflation in *Dosidicus gigas*. Arrows indicate cylinder length (L_c, 0.54 of total mantle length in *D. gigas*), relaxed mantle radius (r_R, recorded during IMR periods in normoxia), contracted mantle radius (r_C) and hyperinflated mantle radius (r_H).

(MC min^{-1}) by video footage analysis. The strength of mantle contraction was calculated as the difference between maximum and minimum mantle diameter (in mm) using ImageJ software (Wayne Rasband, National Institute of Mental Health, Bethesda, MD, USA).

Hyperinflation and stroke volume quantification

During escape jets, squid powerfully contract their radial muscles and, consequently, induce an increase in the outer mantle diameter (between 5% and 10% of relaxed mantle diameter), a process called hyperinflation (represented by the red line in Fig. 2). The relaxed mantle diameter (Fig. 2) was recorded during the IMR periods in normoxia. Changes in the relaxed diameter were determined as a percentage of the relaxed mantle diameter specified at IMR under normoxia.

Stroke volume (V_w, water throughput per mantle contraction) was quantified based on a modified O'Dor (O'Dor, 1988) equation:

$$V_w = [r_H^2 - (r_C - x)^2]\,(0.54\pi\, L) - (0.15M/d_s)\,, \quad (1)$$

where, r_H represents the maximum (hyperinflated) mantle radius (see also Fig. 2), r_C is the contracted mantle radius, x is the mantle thickness (mm), L is the mantle length (the upper mantle is treated as a cylinder of changing diameter, while the lower region is rigid and independent of the mantle radius; in *D. gigas*, cylinder length L_c=0.54L, see Table 3), M is the wet mass (kg), d_s is the squid density (1055 kg m^{-3}) and 0.15 is the correction factor for visceral mass in *D. gigas* (see Table 3).

The ventilatory volume per minute ($\dot{V}_V$, ml min^{-1}) was quantified by multiplying V_w (ml) by ventilatory frequency (MC min^{-1}). The oxygen extraction efficiency (E_{O_2}, %) was quantified *via* the following equations, based on the theoretical model in *I. illecebrosus* (Pörtner, 1994):

$$E_{O_2} = [(\Delta O_2 \times \dot{V}) / \dot{V}_V)] / [(O_{2,IN} \times \dot{V}) / \dot{V}_V]\,, \quad (2A)$$

$$E_{O_2} = \{[(\Delta O_2 - 0.2\Delta O_2) \times \dot{V}) / \dot{V}_V]\} / [(O_{2,IN} \times \dot{V}) / \dot{V}_V]\,, \quad (2B)$$

$$E_{O_2} = \{[(\Delta O_2 - 0.5\Delta O_2) \times \dot{V}) / \dot{V}_V]\} / [(O_{2,IN} \times \dot{V}) / \dot{V}_V]\,, \quad (2C)$$

$$E_{O_2} = \{[(\Delta O_2 - 0.6\Delta O_2) \times \dot{V}) / \dot{V}_V)] / [(O_{2,IN} \times \dot{V}) / \dot{V}_V]\,, \quad (2D)$$

without (Eqn 2A) and with a potential skin respiration contribution (20%, minimum for resting squid, Eqn 2B; 50%, maximum for resting squid, Eqn 2C; and 60%, for squid under exercise, Eqn 2D). Here, ΔO_2 represents the difference between the oxygen flow in and out of the respiratory chamber (μmol l^{-1}), $\dot{V}$ is the flow rate during respiration measurement (l min^{-1}) and $\dot{V}_V$ is the ventilatory volume per minute (ml min^{-1}).

Statistics

Two-way ANOVA were performed to evaluate significant differences between oxygen treatments (21% and 1% O_2), metabolic rates, mantle contraction frequencies and strengths, % of relaxed diameter and stroke volumes. Subsequently, Tukey HSD *post hoc* tests were conducted. In some ventilatory measurements, no data for the late hypoxia treatment were recorded and, as result, independent Student's *t*-tests were applied. Linear and polynomial regressions were performed to assess the correlations between mantle contraction frequency, contraction strength and metabolic rate at different activity levels under control and hypoxic conditions. ANCOVA were conducted to detect significant differences in the relationship between mantle contraction strength/frequency and metabolic rate. For all statistical analysis, STATISTICA (Tulsa, OK, USA) version 10.0 was used.

RESULTS

The effect of hypoxia on *D. gigas* metabolic rate is shown in Fig. 3A. In control animals, activity level only showed significant differences (P<0.05) between IMR and MR_{max}, increasing from 13.7±6.1 to 28.4±12.0 μmol O_2 g^{-1} wet mass h^{-1} (Fig. 3A; supplementary material Table S1). Exposure to severe hypoxia (1% O_2, 1 kPa) led to a significant decrease in O_2 consumption (≤25% of control values, Fig. 3A). AMR and RMR were significantly reduced in EH (exposure time 30–160 min) and IMR at LH (exposure time >180 min; two-way ANOVA, P<0.05; supplementary material Table S1). MR_{max} was only achieved under normoxic conditions and, overall, activity levels (AMR and MR_{max}) declined with hypoxia exposure from 36% to 15% in EH to 0% in LH (Fig. 3A, Fig. 4). RMR dominated in EH treatments, increasing from 47% (normoxia) to 77%, but was not present in LH (100% IMR; Fig. 4). The metabolic scope also changed dramatically with hypoxia (Fig. 3B), decreasing from 15.0±5.9 μmol O_2 g^{-1} wet mass h^{-1} in normoxia to 1.7±0.7 μmol O_2 g^{-1} wet mass h^{-1} in EH, reaching almost 0 (0.3±0.2 μmol O_2 g^{-1} wet mass h^{-1}) in LH (one-way ANOVA,

Table 3. Species-specific correction factors for visceral mass and cylinder mantle length to determine stroke volume in *D. gigas*

N	Wet mass (g)	*L* (cm)	L_c (cm)	CF_{Lc}	V_T (ml)	V_T–V_{vm} (ml)	CF_{vm}
1	10.3	7.2	3.8	0.52	8.5	7.2	0.15
2	6.0	6.0	3.2	0.53	4.5	4.0	0.11
3	5.9	5.9	3.3	0.56	4.0	3.45	0.14
4	6.6	6.2	3.4	0.55	4.5	3.8	0.16
5	5.6	5.4	2.9	0.54	3.0	2.3	0.23
6	10.5	7.0	3.9	0.55	7.3	6.4	0.12
Mean	7.5	6.3	3.4	0.54	5.3	4.5	0.15
s.d.	2.3	0.7	0.4	0.01	2.1	1.9	0.04

L, mantle length; L_c, cylinder mantle length; V_T, total volume (mantle and viscera); V_{vm}, volume of visceral mass. The correction factor for visceral mass (CF_{vm}) was quantified as the proportion of V_{vm} to V_T, and the correction factor for cylinder mantle length (CF_{Lc}) as the proportion of L_c to L.

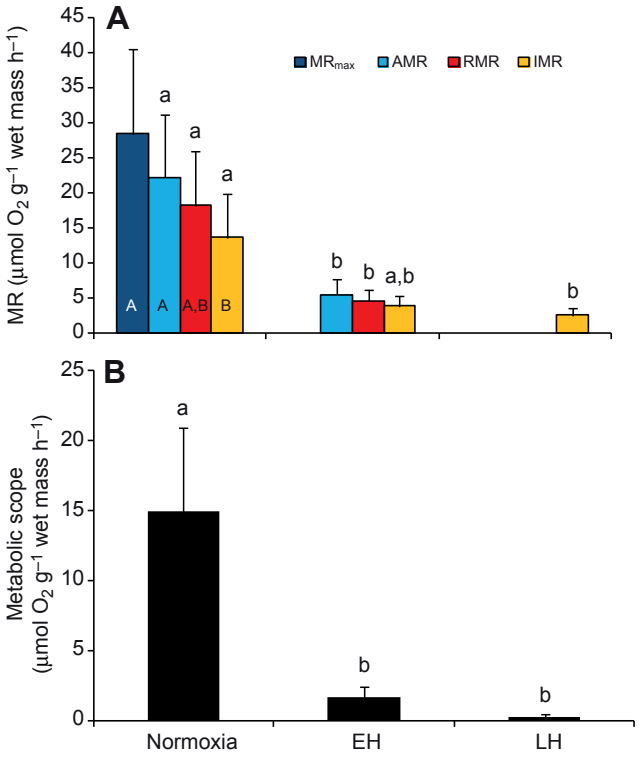

Fig. 3. Effects of hypoxia (1% O_2) on (A) metabolic rate (MR) and (B) metabolic scope (maximum MR–minimum MR) of *D. gigas*. Values are expressed as means and s.d. (*N*=6). EH, early hypoxia; LH, late hypoxia. Significant differences between the level of activity (capital letters) and between treatments (lowercase letters) are indicated (P<0.05, see supplementary material Table S1).

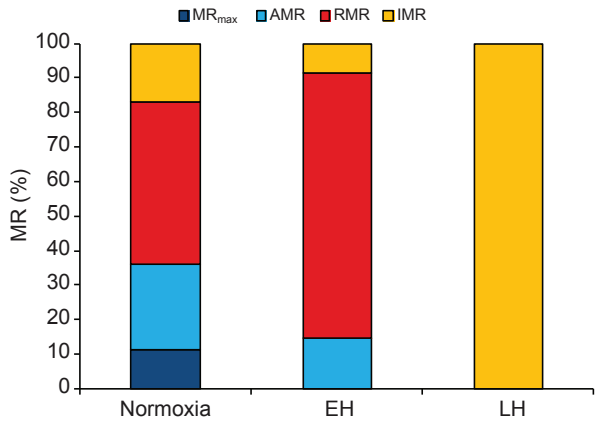

Fig. 4. Changes in IMR, RMR, AMR and MR_{max} of *D. gigas*, under control conditions (21% O_2), and in EH and LH (1% O_2).

F=34.06, P<<0.0001). The number of escape jets per minute increased significantly during AMR from normoxia (11.2 jets min^{-1}) to EH (14.3 jets min^{-1}), but no jets were recorded at LH (Fig. 5A; supplementary material Table S1). Overall (disregarding the activity level), there was a significant decrease in total bursts per hour from normoxia to EH (Fig. 5B, t-test, t=5.55, P<0.05).

All control animals showed a distinct periodicity in oxygen consumption rate (Fig. 1A) and video analysis confirmed that these cycles were correlated with burst frequency and level of activity. Cycles of AMR and MR_{max} differed significantly in length (18±4 and 52±8 min, respectively; Fig. 6A) and frequency (1.5 and 0.2 cycles h^{-1}, respectively; t-test, P<<0.001; Fig. 6B). In early hypoxia, periodicity was also observed (in 5 out of 6 animals, illustrated in Fig. 1B), but with a significantly shorter cycle length (5±1 min; Fig. 6A) and higher frequency (4±1 cycles h^{-1}; Fig. 6B; t-tests, P<0.001).

The effect of hypoxia (1% O_2, 1 kPa) on ventilation rate, a function of mantle contraction frequency and strength, is presented in Fig. 7. Contraction frequency significantly increased with activity, from 45±7 MC min^{-1} in IMR to 74±3 MC min^{-1} in MR_{max} in normoxia, and from 32±6 MC min^{-1} in IMR to 50±5 MC min^{-1} in AMR during EH (Fig. 7A; supplementary material Table S1). During LH, the contraction frequency decreased to 6±3 MC min^{-1}. Contraction strength (Δ mantle diameter; Fig. 7C) increased significantly with metabolic rate in normoxia and EH (supplementary material Table S1). At IMR, mantle contraction strength was more or less constant (around 1.5 mm) during EH, but then decreased dramatically with duration of exposure (LH) down to ≤0.4 mm (two-way ANOVA, P<0.05; supplementary material Table S1). The correlations between contraction frequency/strength and metabolic rate are given in Fig. 7B,D. In both cases, the relationship is linear for both normoxic (Fig. 7B: R^2=0.977, F=130.3, P=0.001; Fig. 7D: R^2=0.982, F=167.6, P<0.001) and hypoxic treatments (Fig. 7B: R^2=0.850, F=17, P<0.05; Fig. 7D: R^2=0.855, F=17.7, P<0.05). Interestingly, the slope for hypoxia is significantly steeper (F=12.8, P<0.01, frequency; F=5.2, P<0.05, strength) than that for normoxia, indicating that much higher ventilation rates (frequency and strength) are required to achieve even modest metabolic rates during exposure to hypoxia. There was also a significant correlation between mantle contraction frequency and strength (Fig. 8). Under normoxic conditions, squid showed a linear relationship between strength and frequency (R^2=0.993, P<<0.001), whereas under hypoxia (1% O_2, 1 kPa) the relationship was polynomial (R^2=0.988, P=0.01), indicating reduced relative ventilation frequency.

There was a significant increase in the percentage relaxed mantle diameter in AMR and MR_{max} (i.e. hyperinflation) under normoxia (Fig. 9; supplementary material Table S1). However, the opposite trend was observed in EH and LH.

The effect of hypoxia on ventilation stroke volume V_w is shown in Fig. 10A. The highest value was observed during maximum activity (MR_{max}) under normoxia (4.8 ml). During EH, there was a significant increase in V_w, with activity ranging from 2.7 ml (IMR) to 3.6 ml (RMR) to 4.3 ml (AMR; P<0.05). In LH, there was a significant drop (42%) during the inactive state (IMR). By multiplying the V_w (Fig. 10A) by ventilation (contraction) frequency (Fig. 7A), we obtained the ventilatory volume per minute $\dot{V}_V$ (Fig. 10B). As a result, it became evident that in EH the increase in V_w (at AMR and RMR; Fig. 10A) was followed by a decrease in contraction frequency (Fig. 7A), leading to similar values of $\dot{V}_V$ in normoxia and EH (Fig. 10B). In LH, this ventilatory parameter was significantly lower (Fig. 10B, P<0.05; supplementary material Table S1). Oxygen extraction efficiency E_{O_2} under normoxia ranged between 6.4% and 13.4% (2.6% and 5.4%, taking into account 60% potential skin respiration) from IMR to MR_{max} and was significantly elevated as a result of exposure to hypoxia, with a minimum of 43.7% (15.2% including 60% cutaneous uptake) in IMR during LH, and a maximum of 81.5% (33.6%) in AMR during EH (Fig. 10C,D, P<0.05; supplementary material Table S1). In Table 4, E_{O_2} without, and with 20%, 50% and 60% potential skin respiration is presented.

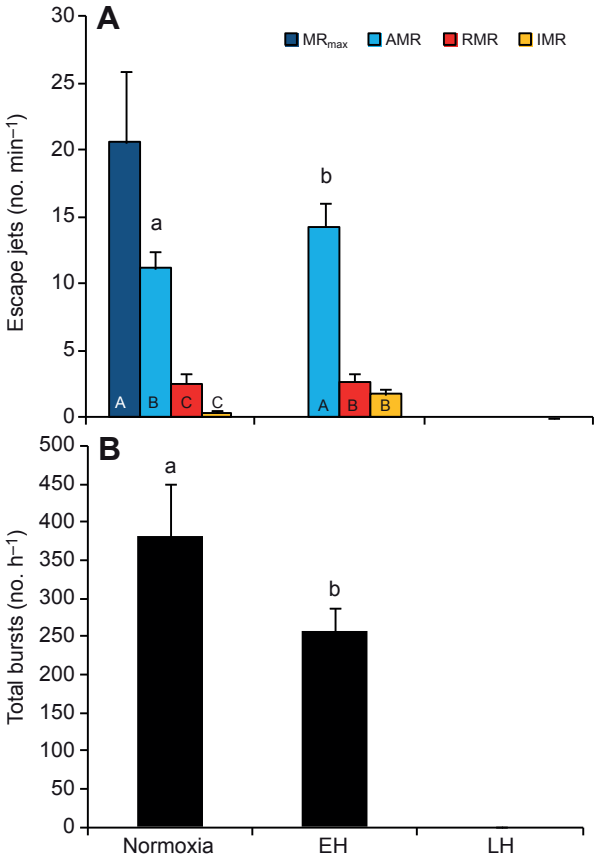

Fig. 5. Effect of hypoxia (1% O_2) on burst frequency in *D. gigas*. (A) Number of escape jets per minute during IMR, RMR, AMR and MR_{max}, and (B) total number of burst events per hour. Values are expressed as means ± s.d. (*N*=6). Significant differences between active and maximum active cycles (capital letters) and between oxygen treatments (lowercase letters) are indicated (*P*<0.05).

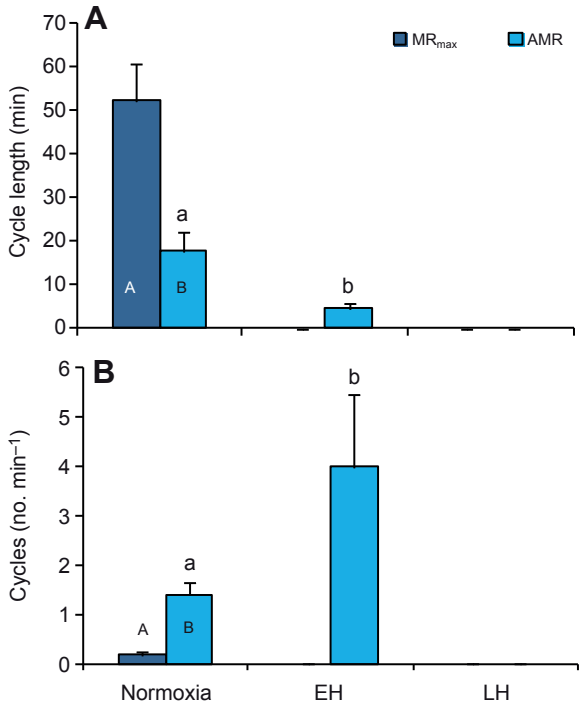

Fig. 6. Effect of hypoxia (1% O_2) on the periodicity of activity cycles in *D. gigas*. (A) Average cycle length for MR_{max} and AMR, and (B) cycle frequency. Values are expressed as means and s.d. (*N*=5; 1 of the 6 was not cycling). Significant differences between AMR and MR_{max} cycles (capital letters) and between oxygen treatments (lowercase letters) are indicated (*P*<0.05).

DISCUSSION

Effect of hypoxia on metabolic rate and metabolic scope

Dosidicus gigas metabolic rate varied between 14 and 29 μmol $O_2\,g^{-1}$ wet mass h^{-1}, depending on the level of activity. These values were in agreement with those from our previous studies (Rosa and Seibel, 2008; Rosa and Seibel, 2010), which also indicated a wide metabolic scope in well-oxygenated water. *Dosidicus gigas* is able to maintain these high metabolic rates down to an ambient O_2 level of ~20 μmol l^{-1} (~2 kPa, ~200 m depth) (Gilly et al., 2006), below which they dramatically drop. In the present experiments, with the temperature and oxygen conditions found in the OMZ, squid metabolic rate dropped more than 75% under exposure to early hypoxia with no further significant reduction with exposure time. Moreover, MR_{max} was not recorded under such conditions and the metabolic scope was significantly decreased (Fig. 1B, Fig. 3B, Fig. 4). In general, organisms suppress their metabolism by 50–95% by shutting down expensive processes (i.e. protein synthesis, muscle activity) (Guppy and Withers, 1999) and supplement the remaining energy demand using a combination of available O_2 and anaerobic metabolic pathways (Seibel, 2011). Cephalopods that routinely depend on jet propulsion extract only a small proportion (5–10%) of the available O_2 from the ventilatory stream, but are able to alter the O_2 extraction efficiency (≤25%) when necessary, including cutaneous respiration, for example (Wells et al., 1988; Wells and O'Dor, 1991; Pörtner, 1994). Yet, the most common strategy among powerful predators that managed to minimize the trade-offs between high performance and hypoxia tolerance is a high-affinity respiratory protein (Lowe et al., 2000; Gilly et al., 2006; Seibel, 2011). Hemocyanin of cephalopods is usually characterized by a low O_2 affinity with high pH sensitivity, properties that facilitate O_2 release to demanding tissues, but presumably interfere with O_2 extraction from hypoxic or CO_2-rich seawater (Pörtner, 1994; Pörtner, 2002; Melzner et al., 2007). Yet, it has been reported (Seibel, 2012) that the respiratory protein in *D. gigas* is both highly temperature and pH sensitive, but, in addition, is characterized by a high O_2-binding affinity. These properties facilitate O_2 uptake in cold, deep waters where O_2 is scarce and enhances O_2 release in warmer surface waters where O_2 and O_2 demand are elevated. Furthermore, Seibel (Seibel, 2012) could link the hypoxia tolerance down to P_{crit} (1.6 kPa, 10°C) (Trueblood and Seibel, 2012) to the optimized hemocyanin function in *D. gigas*, and suggests that below P_{crit} (~170 m, Gulf of California) the onset of metabolic suppression kicks in.

However, metabolic suppression is time limited, as anaerobic glycolysis results in the accumulation of protons (H^+) and organic compounds such as lactate and octopine (Hochachka and Somero, 2002; Rosa and Seibel, 2010) with harmful consequences on acid–base status (Hochachka and Mommsen, 1983). Recent biochemical analysis revealed that under EH ~60% of the depressed metabolism is still achieved aerobically but this drops to ~45% at LH (K.T., unpublished). No significant further drop in metabolic rate between EH and LH could be quantified, indicating a limitation in the potential to suppress metabolism and a possible switch in

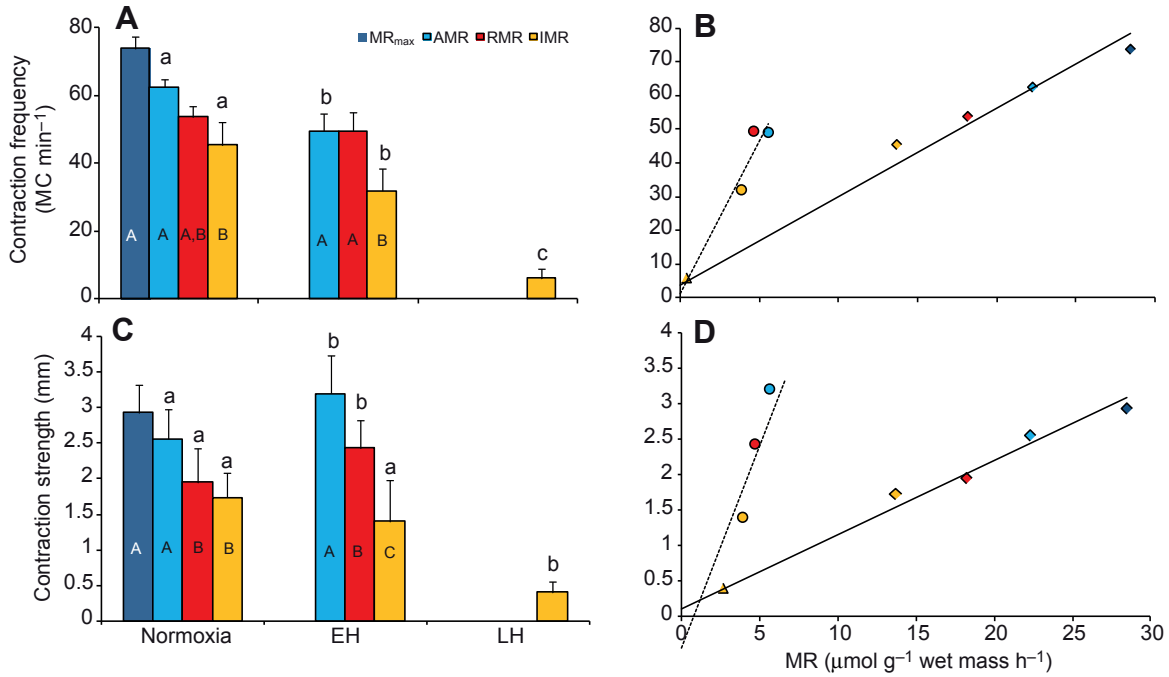

Fig. 7. Effect of hypoxia (1% O_2) on ventilation rates of *D. gigas*. (A) Mantle contraction (MC) frequency, and (C) mantle contraction strength (change in mantle diameter). Significant differences between activity levels (capital letters) and between treatments (lowercase letters) are indicated (P<0.05, see supplementary material Table S1). Values are expressed as means and s.d. (N=6). (B,D) Ventilation frequency and strength, plotted against oxygen consumption. Diamonds, normoxia; circles, EH; triangles, LH. Yellow, IMR; red, RMR; bright blue, AMR; dark blue, MR_{max}.

energy expenditure from muscle activity to acid–base and ion regulation processes.

Vertical migrations and respiratory cycling behavior

Jumbo squid are diel vertical migrators that spend their nights in shallower, well-oxygenated waters (~70 m) and dive into the OMZ during the day (peak depth range 200–300 m; 2–0.2 kPa) (Gilly et al., 2006) (Trueblood and Seibel, 2012). Thereby, jumbo squid spend more than 70% of the day below 200 m (≤2% O_2, 2 kPa) (Gilly et al., 2006) following their main prey (myctophid fishes) (Markaida and Sosa-Nishizaki, 2003; Markaida et al., 2008) and in this way also escape from: (i) unfavorable warmer sea surface temperatures, and (ii) elevated predation pressure and resource (food) competition, as most active fish predators are excluded from the OMZ (Prince and Goodyear, 2006).

Nonetheless, acoustic data revealed short-term cyclic vertical movements (~15–90 min), during day and night time, that have been interpreted as active forages (Gilly et al., 2006). In a previous study, we (Rosa and Seibel, 2010) discovered a similar periodicity in the rate of metabolism in the confines of a respiration chamber (cycle length ~20 min), which was also observed in the present experiments (20/60 min for active/maximum active cycles; Fig. 1A, Fig. 6A). As the frequency and duration of brief vertical movements are similar to the periodicity reported here, we argue that the activity cycles (MR_{max} and AMR) at normoxia may reflect the capacity to perform migratory forays.

During early hypoxia, the respiratory cycles were shorter in length but increased in frequency (Fig. 1B, Fig. 6). This was accompanied by an increase in the number of escape jets in active periods (see AMR in Fig. 5A) and a faster switch between swimming modes (data not shown). As high muscular activity involves the use of anaerobic ATP production, cycling between aerobic and anaerobic swimming phases over short time intervals may reduce the cost of transport and permit a long-term use of anaerobic resources, a strategy that in the long term may imply a maximized use of ambient O_2 (Finke et al., 1996). Finke and colleagues assumed that this oscillation between periods of high and low muscular activity may have been related to the hypoxia tolerance of *Lolliguncula brevis* in coastal waters. It is plausible that *D. gigas* uses the same strategy. Furthermore, it displayed an enhanced usage of its lateral fins under progressive hypoxia, with a peak at the transition from EH to LH (data not shown). This also might contribute to minimize the costs of transport, as lateral fins can push a large mass of water especially at low velocities (O'Dor et al., 1988; Wells and O'Dor, 1991). At LH (onset ~170±10 min),

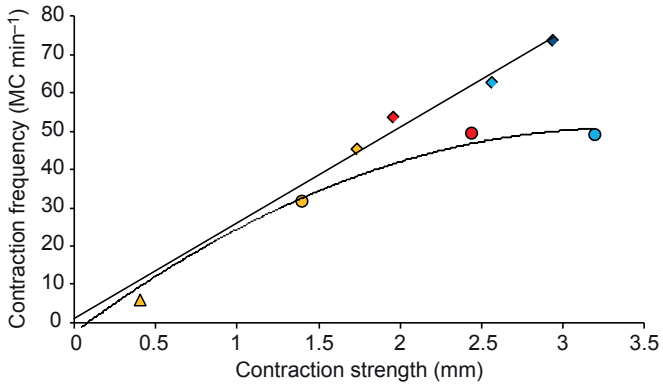

Fig. 8. Relationship between mantle contraction (MC) strength (change in mantle diameter) and frequency (ventilation rate) in *D. gigas* under normoxia and hypoxia (1% O_2). The black straight line and diamonds represent normoxia, the dashed line represents hypoxia, with circles for EH and triangles for LH. Yellow, IMR; red, RMR; bright blue, AMR; dark blue, MR_{max}. Values are expressed as means (N=6).

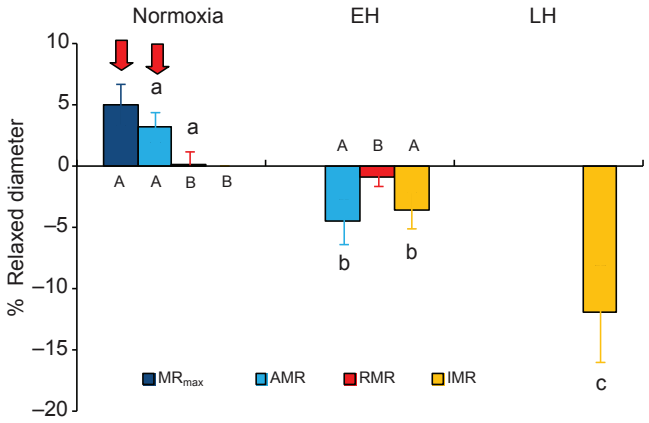

Fig. 9. Changes in the relaxed mantle diameter of IMR, RMR, AMR and MR_{max} in *D. gigas*, under control conditions (21% O_2), EH and LH (1% O_2). Percentage relaxed mantle diameter was calculated based on the relaxed diameter under IMR normoxia. Values are expressed as means and s.d. (*N*=6). Red arrows indicate a hyperinflation mechanism. Significant differences between active and maximum active cycles (capital letters) and between oxygen treatments (lowercase letters) are indicated (P<0.05).

jumbo squid moved into a lethargic state and ventilatory cycles stopped (Fig. 1C, Fig. 6). This lethargic behavior has been associated with metabolic suppression (Rosa and Seibel, 2010). Gilly and colleagues (Gilly et al., 2006) claimed that a substantial number of excursions lasted for many hours (maximum duration of 400/800 min below 300/200 m), during which time rhythmic diving occurred that appeared to be as robust as that observed at well-oxygenated, shallower depths. The majority of these extended dives at 300 m (~1% O_2, 1 kPa) peaked between 140 and 240 min, which is in close agreement with the onset of late hypoxia (~170±10 min) in the present study. Yet, the switch to severe hypoxia within the respiration chambers could have been faster than during average, natural descents [see fig. 11 of Gilly (Gilly et al., 2006)], even though fast migrations (i.e. hunting, escape) in jumbo squid are known, which might have elevated stress. Also the lack of food within the chambers might have accelerated the depletion of anaerobic energy reserves, resulting in the onset of lethargy.

Ventilatory mechanisms and oxygen extraction efficiency during hypoxia

In normoxia, the *D. gigas* mantle contraction frequency and strength were linearly correlated (Fig. 8) and increased significantly with activity level (Figs 7, 8). Additionally, an increased stroke volume and ventilatory volume per minute (Fig. 10) were observed, followed by a hyperinflation process during high activity periods (red arrows in Fig. 9). The squid *Illex illecebrosus* and *L. opalescens*, in contrast, do not vary their ventilation *via* frequency with vigorous jetting, but *via* powerful contractions of their circular fibres (Wells et al., 1988; Webber and O'Dor, 1985). A linear increase in ventilation frequency with speed (<0.6 m s^{-1}) was found in *I. illecebrosus*, but at speeds >0.6 m s^{-1} the correlation was linear with cavity pressure (Webber and O'Dor, 1986). As a result, *I. illecebrosus* and *L. opalescens* seem to be restricted to regulating ventilation strength and frequency at the same time, while *D. gigas* seems to have developed an optimized fine-tuning between locomotion and ventilation, and seems to have the potential to regulate mantle contraction frequency, strength and stroke volume according to activity.

Yet, EH changed the relationship between ventilation strength and frequency from linear to polynomial with increasing activity

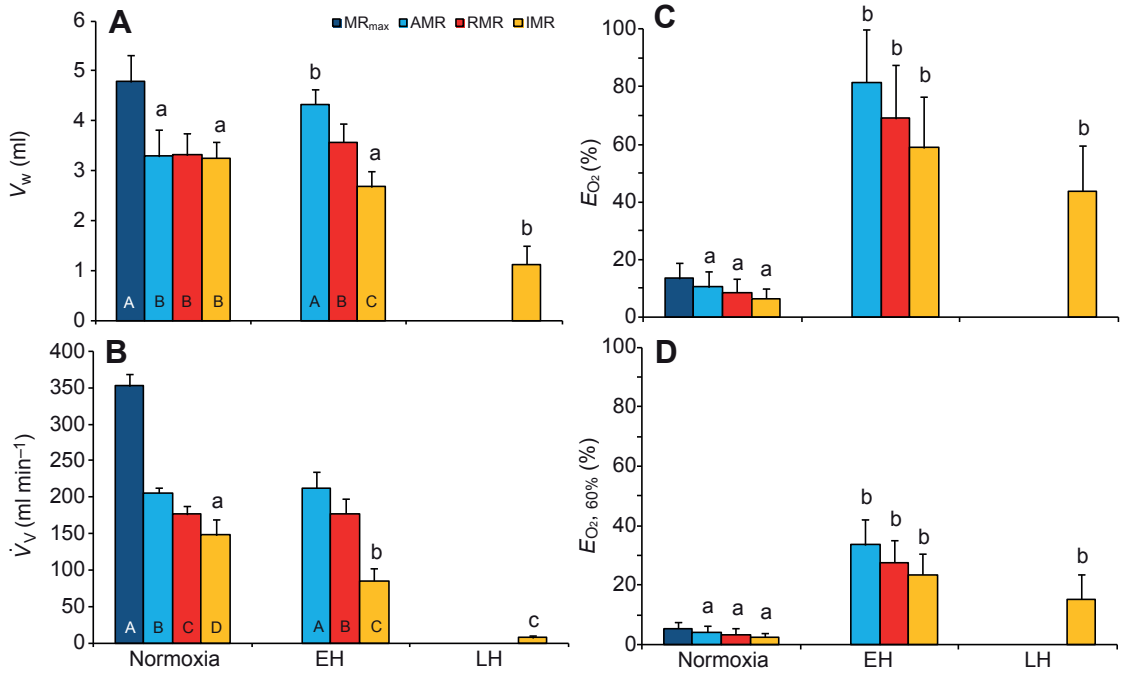

Fig. 10. Changes in (A) stroke volume V_w, (B) ventilatory volume per minute $\dot{V}_V$, (C) O_2 extraction efficiency E_{O_2} and (D) O_2 extraction efficiency with potential skin respiration contribution ($E_{O_2,60\%}$) in IMR, RMR, AMR and MR_{max} of *D. gigas*, under control conditions (21% O_2), EH and LH (1% O_2). Values are expressed as means and s.d. (*N*=6). Significant differences between active and maximum active cycles (capital letters) and between oxygen treatments (lowercase letters) are indicated (P<0.05).

Table 4. Oxygen extraction efficiencies without (0%) and with (20%, 50% and 60%) consideration of potential skin respiration

Treatment	Activity	Skin respiration			
		0%	20%	50%	60%
Normoxia	MR_{max}	13.4±5.4	10.7±4.3	6.7±2.7	5.3±2.1
	AMR	10.5±5.4	8.4±4.4	5.2±2.7	4.2±2.2
	RMR	8.6±4.7	6.9±3.8	4.3±2.4	3.4±1.9
	IMR	6.4±3.4	5.1±2.7	3.2±1.7	2.6±1.4
EH	AMR	81.5±18.3	67.3±16.9	41.9±10.6	33.5±8.5
	RMR	69.1±18.4	55.3±14.7	34.5±9.2	27.6±7.4
	IMR	58.8±17.7	47.1±14.2	29.4±8.9	23.5±7.1
LH	IMR	43.7±16.0	35.0±12.8	19.0±10.6	15.2±8.5

Data (means ± s.d.) are for inactive, routine, active and maximum active levels (IMR, RMR, AMR and MR_{max}) in *D. gigas*, under control conditions (21% O_2), and in early and late hypoxia (1% O_2). Here, 20% skin respiration represents the minimum resting value, 50% the maximum resting value and 60% the cutaneous uptake under exercise in squid (*I. illecebrosus*, theoretical model) (Pörtner, 1994). EH, early hypoxia; LH, late hypoxia (>180 min).

(Fig. 8). This indicates that *D. gigas*, under hypoxic conditions, primarily increases the power of mantle contraction and does not regulate its frequency, as was observed for *I. illecebrosus* and *L. opalescens* under normoxia (Wells et al., 1988).

In EH, jumbo squid showed a larger inflation period leading to reduced contraction frequency and decreased relaxed mantle diameter, which optimize O_2 uptake (i.e. shorter diffusion ways) *via* gills and skin (see Fig. 10C). Additionally, they seem to breathe 'deeply', with more powerful contractions (see different slopes in Fig. 7D) and enhanced stroke volume (Fig. 10A). This deep-breathing behavior allows the squid to have the same amount of water passing through the gills per period of time, i.e. a stable ventilatory volume per minute, and explains the maintenance of the squid's cycling activity under such O_2 conditions.

The O_2 extraction efficiency reached ~82% in EH at active metabolic rates (Fig. 10C) without consideration of cutaneous uptake. Other cephalopods, such as nautilus and squid (*L. brevis*), also alter the effectiveness of oxygen extraction (i.e. cutaneous uptake) from the ventilatory stream as a result of falling ambient O_2 levels or exercise when necessary, but at around 15–20% (once 43% in nautilus) (Wells et al., 1988; Wells, 1990; Pörtner, 1994). Maximum O_2 extraction efficiency (AMR at EH), considering 60% potential skin respiration in squid (theoretical model, *I. illecebrosus* under exercise) (Pörtner, 1994), was still found to be 34% in our study (Fig. 10D). The organization of squid mantle muscle structure (mitochondria-rich inner and outer layer) supports the importance of skin respiration in cephalopods (Gosline and DeMont, 1985). Under hypoxia, P_{O_2} gradients drastically decline and therefore do not favor diffusion processes (O_2 uptake *via* skin and gills). Under LH, when jumbo squid cease swimming, cutaneous uptake might even decrease as a result of a lack of convection. Deep-breathing behavior observed at EH, instead, might favour cutaneous uptake (inner and outer mantle), but here we were not able to distinguish between O_2 uptake *via* skin and gills.

In cuttlefish and octopus, organisms that are less dependent on jet propulsion, the fraction of oxygen extraction from the ventilatory stream is higher [50–90% in cuttlefish (Melzner et al., 2006); 45–75% in octopus (Wells and Wells, 1985; Wells, 1990)], and their O_2 uptake can only be enhanced by an elevation in water throughput and increased diffusion gradients at the water–blood threshold (Melzner et al., 2006). Other OMZ residents in the Gulf of California, like *Gnathophausia ingens*, can regulate oxygen uptake mainly *via* an increase in ventilation volume (5–6 times, maximum 8) at constant (or slightly increasing) O_2 extraction efficiencies that can reach 48–60%, with a maximum ~95% (Childress, 1971). However, these large changes in ventilation volume are not possible for squid because of the constraints imposed by the massive collagenous tissues in the mantle walls of muscular squid (Gosline and Shadwick, 1983; Wells et al., 1988).

In contrast, at LH, all the ventilatory processes were significantly reduced, except for O_2 extraction efficiency followed by a lethargic state. Also, Boutilier and colleagues (Boutilier et al., 1996) reported that *Nautilus* cease ventilatory movements, cardiac output and heartbeat to survive prolonged periods of hypoxia. In the majority of investigated squid, ventilation was completely shut down, but we cannot rule out the possibility that there were further very weak contractions that could not be assessed by the method of analysis used. Another explanation could be that *D. gigas* has the potential to uncouple its ventilatory and locomotory mechanisms *via* a collar flap system, as is known for resting sepia and to some extent for squid (Bone et al., 1994). This original respiratory design of cephalopods (Wells, 1988) drives expiration *via* an active inward movement of the collar flaps (and probably *via* stored elastic energy during inhalation) (Gosline and Shadwick, 1983) without the activity of circular muscle fibers (Bone et al., 1994).

Unfortunately, the experiments were interrupted a maximum of 20 min after the jumbo squid stopped moving. Nonetheless, recent data suggest that juvenile (R.R., unpublished) and adult jumbo squid (B.A.S., unpublished) can sustain severe hypoxia (1% O_2) for at least 6–12 h and therefore might use lethargy as a strategy to extend the residence time in the OMZ. It is noteworthy that our experiments were conducted with juveniles and therefore our results might not apply in adults, even though metabolic rates in juvenile and adult squid should not differ, as muscular squid display an unusual scaling relationship (tendency to isometry). This might be a consequence of: (1) tubular geometry (mantle diameter increases faster than thickness with growth), exchange surfaces (surface area$^{1/2}$:volume$^{1/3}$ increases with size) (O'Dor and Hoar, 2000) and cutaneous respiration (~60%) (Pörtner, 1994; Pörtner, 2002); (2) ontogenetic differences in locomotory expenditure, because the squid cost of transport may not decrease as much with size as that in other animals (e.g. mammals, birds and fish), where adults are more energy efficient; and (3) energetic requirements during all stages of the squid's short life cycle (namely, for growth and reproduction). High sustained production costs during all ages may result in a *B* value (scaling coefficient) that does not decrease with increasing body mass (Seibel, 2007; Rosa et al., 2009). However, it remains unclear whether adults will adjust their ventilatory mechanisms to low oxygen levels in a similar way to juveniles, especially as little is known about the potential of oxygen uptake *via* the skin under hypoxia.

LIST OF SYMBOLS AND ABBREVIATIONS

AMR	active metabolic rate
d_s	squid density
E_{O_2}	O_2 extraction efficiency
IMR	inactive metabolic rate
L	mantle length
L_c	cylinder length
M	weight mass (kg)
MC	mantle contractions
MR	metabolic rate
MR_{max}	maximum active metabolic rate
OMZ	oxygen minimum zone
r_C	contracted mantle radius
r_H	maximum (hyperinflated) mantle radius
RMR	routine metabolic rate
$\dot{V}$	flow rate
$\dot{V}_V$	ventilatory volume per minute
V_w	stroke volume
x	mantle thickness (mm)

ACKNOWLEDGEMENTS

We would like to thank Unai Markaida for his assistance with collection of the specimens.

FUNDING

This work was supported by research grants to R.R. from the Portugal–US Research Networks Program (FLAD/US National Science Foundation Research Grant) and The Portuguese Foundation for Science and Technology (FCT, Ciência 2007 Program) and to B.A.S. from the National Science Foundation [grant OCE-0851043].

REFERENCES

Abitía-Cárdenas, L., Muhlia-Melo, A., Cruz-Escalona, V. and Galván-Magaña, F. (2002). Trophic dynamics and seasonal energetics of striped marlin *Tetrapturus audax* in the southern Gulf of California, Mexico. *Fish. Res.* **57**, 287-295.

Bartol, I. K. (2001). Role of aerobic and anaerobic circular mantle muscle fibers in swimming squid: electromyography. *Biol. Bull.* **200**, 59-66.

Bone, Q., Brown, E. R. and Travers, G. (1994). On the respiratory flow in the cuttlefish *Sepia officinalis*. *J. Exp. Biol.* **194**, 153-165.

Boutilier, R. G., West, T. G., Pogson, G. H., Mesa, K. A., Wells, J. and Wells, M. J. (1996). Nautilus and the art of metabolic maintenance. *Nature* **382**, 534-536.

Brill, R. W. (1994). A review of temperature and oxygen tolerance studies of tunas pertinent to fisheries oceanography, movement models and stock assessments. *Fish. Oceanogr.* **3**, 204-216.

Brill, R. W. (1996). Selective advantages conferred by the high performance physiology of tunas, billfishes, and dolphin fish. *Comp. Biochem. Physiol.* **113**, 3-15.

Childress, J. J. (1971). Respiratory adaptations to the oxygen minimum layer in the bathypelagic mysid *Gnathophausia ingens*. *Biol. Bull.* **141**, 109-121.

Childress, J. J. and Mickel, T. J. (1980). A motion compensated shipboard precision balance system. *Deep Sea Res.* **27**, 965-970.

Clarke, A. and Paliza, O. (2001). The food of sperm whales in the southeast Pacific. *Mar. Mamm. Sci.* **17**, 427-429.

Finke, E., Pörtner, H. O., Lee, P. G. and Webber, D. M. (1996). Squid (*Lolliguncula brevis*) life in shallow waters: oxygen limitation of metabolism and swimming performance. *J. Exp. Biol.* **199**, 911-921.

Gilly, W. F., Markaida, U., Baxter, C. H., Block, B. A., Boustany, A., Zeidberg, L., Reisenbichler, K., Robison, B., Bazzino, G. and Salinas, C. (2006). Vertical and horizontal migrations by the jumbo squid *Dosidicus gigas* revealed by electronic tagging. *Mar. Ecol. Prog. Ser.* **324**, 1-17.

Gosline, J. M. and DeMont, M. E. (1985). Jet-propelled swimming in squids. *Sci. Am.* **252**, 96-103.

Gosline, J. M. and Shadwick, R. E. (1983). The role of elastic energy storage mechanisms in swimming; an analysis of mantle elasticity in escape jetting in the squid *Loligo opalescens*. *Can. J. Zool.* **61**, 1421-1431.

Gosline, J. M., Steeves, J. D., Harman, A. D. and DeMont, M. E. (1983). Patterns of circular and radial mantle muscle activity in respiration and jetting of the squid *Loligo opalescens*. *J. Exp. Biol.* **104**, 97-109.

Guppy, M. and Withers, P. (1999). Metabolic depression in animals: physiological perspectives and biochemical generalizations. *Biol. Rev. Camb. Philos. Soc.* **74**, 1-40.

Hochachka, P. W. and Mommsen, T. P. (1983). Protons and anaerobiosis. *Science* **219**, 1391-1397.

Hochachka, P. W. and Somero, G. N. (2002). *Biochemical Adaptation: Mechanism and Process in Physiological Evolution*. Oxford: Oxford University Press.

Ichii, T., Mahapatra, K., Watanabe, T., Yatsu, A., Inagake, D. and Okada, Y. (2002). Occurrence of jumbo flying squid *Dosidicus gigas* aggregations associated with the countercurrent ridge off the Costa Rica Dome during 1997 El Niño and 1999 La Niña. *Mar. Ecol. Prog. Ser.* **231**, 151-166.

Kamykowski, D. and Zentara, S.-J. (1990). Hypoxia in the world ocean as recorded in the historical data set. *Deep Sea Res. Part II Top. Stud. Oceanogr.* **37**, 1861-1874.

Lowe, T. E., Brill, R. W. and Cousins, K. I. (2000). Blood oxygen-binding characteristics of low ambient oxygen. *Mar. Biol.* **136**, 1087-1098.

Markaida, U. and Sosa-Nishizaki, O. (2003). Food and feeding habits of jumbo squid *Dosidicus gigas* (Cephalopoda: Ommastrephidae) from the Gulf of California, Mexico. *J. Mar. Biol. Assoc. UK* **83**, 507-522.

Markaida, U., Rosenthal, J. J. C. and Gilly, W. F. (2005). Tagging studies on the jumbo squid (*Dosidicus gigas*) in the Gulf of California, Mexico. *Fish Bull.* **103**, 219-226.

Markaida, U., Salinas-Zavala, C. A., Rosas-Luis, R., Booth, F., Ashley, T. and Gilly, W. F. (2008). Food and feeding of jumbo squid *Dosidicus gigas* in the central Gulf of California during 2005-2007. *CalCOFi Rep.* **49**, 90-103.

Melzner, F., Bock, C. and Pörtner, H. O. (2006). Temperature-dependent oxygen extraction from the ventilatory current and the costs of ventilation in the cephalopod *Sepia officinalis*. *J. Comp. Physiol. B* **176**, 607-621.

Melzner, F., Mark, F. C. and Pörtner, H. O. (2007). Role of blood-oxygen transport in thermal tolerance of the cuttlefish, *Sepia officinalis*. *Integr. Comp. Biol.* **47**, 645-655.

Morrison, J. M., Dodispoti, L. A., Smith, S. L., Wishner, K., Flagg, C., Gardner, W. D., Gaurin, S., Naqvi, S. W. A., Manghnani, V., Prosperie, L. et al. (1999). The oxygen minimum zone in the Arabian Sea during 1995 – overall seasonal and geographic patterns and relationship to oxygen gradients. *Deep Sea Res. Part II Top. Stud. Oceanogr.* **46**, 1903-1931.

Nasby-Lucas, N., Dewar, H., Lam, C. H., Goldman, K. J. and Domeier, M. L. (2009). White shark offshore habitat: a behavioral and environmental characterization of the eastern Pacific shared offshore foraging area. *PLoS ONE* **4**, e8163.

Nesis, K. N. (1983). *Dosidicus gigas. Cephalopod Life Cycles, Species Accounts*. London: Academic Press.

Nigmatullin, C. M., Nesis, K. N. and Arkhipkin, A. I. (2001). A review on the biology of the jumbo squid *Dosidicus gigas*. *Fish. Res.* **54**, 9-19.

O'Dor, R. K. (1988). The forces acting on swimming squid. *J. Exp. Biol.* **137**, 421-442.

O'Dor, R. K. and Hoar, J. A. (2000). Does geometry limit squid growth? *ICES J. Mar. Sci.* **57**, 8-14.

Pörtner, H. O. (1994). Coordination of metabolism, acid-base regulation and haemocyanin function in cephalopods. *Mar. Freshw. Behav. Physiol.* **25**, 131-148.

Pörtner, H. O. (2002). Environmental and functional limits to muscular exercise and body size in marine invertebrates athletes. *Comp. Biochem. Physiol.* **133**, 303-321.

Prince, E. D. and Goodyear, C. P. (2006). Hypoxia-based habitat compression of tropical pelagic fishes. *Fish. Oceanogr.* **15**, 451-464.

Rodhouse, P. G., Waldua, C. M., Morales-Bojórquez, E. and Hernández-Herrera, A. (2006). Fishery biology of the Humboldt squid, *Dosidicus gigas*, in the Eastern Pacific Ocean. *Fish. Res.* **79**, 13-15.

Rosa, R. and Seibel, B. A. (2008). Synergistic effects of climate-related variables suggest future physiological impairment in a top oceanic predator. *Proc. Natl. Acad. Sci. USA* **105**, 20776-20780.

Rosa, R. and Seibel, B. A. (2010). Metabolic physiology of the Humboldt squid, *Dosidicus gigas*: implications for vertical migration in a pronounced oxygen minimum zone. *Prog. Oceanogr.* **86**, 72-80.

Rosa, R., Trueblood, L. and Seibel, B. A. (2009). Ecophysiological influence on scaling of aerobic and anaerobic metabolism of pelagic gonatid squids. *Physiol. Biochem. Zool.* **82**, 419-429.

Ruiz-Cooley, R. I., Gendron, D., Aguíñiga, S., Mesnick, S. and Carriquiry, J. D. (2004). Trophic relationships between sperm whales and jumbo squid using stable isotopes of C and N. *Mar. Ecol. Prog. Ser.* **277**, 275-283.

Seibel, B. A. (2007). On the depth and scale of metabolic rate variation: scaling of oxygen consumption rates and enzymatic activity in the Class Cephalopoda (Mollusca). *J. Exp. Biol.* **210**, 1-11.

Seibel, B. A. (2011). Critical oxygen levels and metabolic suppression in oceanic oxygen minimum zones. *J. Exp. Biol.* **214**, 326-336.

Seibel, B. A. (2012). The jumbo squid, *Dosidicus gigas* (Ommastrephidae), living in oxygen minimum zones II: blood-oxygen binding. *Deep Sea Res. Part II Top. Stud. Oceanogr.* http://dx.doi.org/10.1016/j.dsr2.2012.10.003.

Stramma, L., Prince, E. D., Schmidtko, S., Jiangang, L., Hoolihan, J. P., Visbeck, M., Wallace, D. W. R., Brandt, P. and Körtzinger, A. (2012). Expansion of oxygen minimum zones may reduce available habitat for tropical pelagic fishes. *Nat. Clim. Chang.* **2**, 33-37.

Trueblood, L. A. and Seibel, B. A. (2012). The jumbo squid, *Dosidicus gigas* (Ommastrephidae), living in oxygen minimum zones I: oxygen consumption rates and critical oxygen partial pressures. *Deep Sea Res. Part II Top. Stud. Oceanogr.* http://dx.doi.org/10.1016/j.dsr2.2012.10.004.

Vetter, R., Kohin, S., Preti, A., McClatchie, S. and And Dewar, H. (2008). Predatory interactions and niche overlap between mako shark, *Isurus oxyrinchus*, and jumbo squid, *Dosidicus gigas*, in the California Current. *CCOFI Rep.* **49**, 142-156.

Waluda, C. M. and Rodhouse, P. G. (2006). Remotely sensed mesoscale oceanography of the Central Eastern Pacific and recruitment variability in *Dosidicus gigas*. *Mar. Ecol. Prog. Ser.* **310**, 25-32.

Webber, D. M. and O'Dor, R. K. (1985). Respiration and swimming performance of short-finned squid (*Illex illecebrosus*). *NAFO Sci. Coun. Studies* **9**, 133-138.

Webber, D. M. and O'Dor, R. K. (1986). Monitoring the metabolic rate and activity of free-swimming squid with telemetered jet pressure. *J. Exp. Biol.* **126**, 205-224.

Webber, D. M., Aitken, J. P. and O'Dor, R. K. (2000). Costs of locomotion and vertic dynamics of cephalopods and fish. *Physiol. Biochem. Zool.* **73**, 651-662.

Wells, M. J. (1988). The mantle muscle and mantle cavity of cephalopods. In *The Mollusca, Form and Function*, Vol. 11 (ed. E. R. Trueman and M. R. Clarke), pp. 287-300. San Diego, CA: Academic Press.

Wells, M. J. (1990). Oxygen extraction and jet propulsion in cephalopods. *Can. J. Zool.* **68**, 815-824.

Wells, M. J. and O'Dor, R. K. (1991). Jet propulsion and the evolution of the cephalopods. *Bull. Mar. Sci.* **49**, 419-432.

Wells, M. J. and Wells, J. (1985). Ventilation frequencies and stroke volumes in acute hypoxia in octopus. *J. Exp. Biol.* **118**, 445-448.

Wells, M. J., Hanlon, R. T., Lee, P. G. and Dimarco, F. P. (1988). Respiratory and cardiac performance in *Lolliguncula brevis* (Cephalopoda, Myopsida): the effects of activity, temperature and hypoxia. *J. Exp. Biol.* **138**, 17-36.

Table S1. Results of two-way ANOVA evaluating the effects of early and late hypoxia (1% O_2) on metabolic rate (μmol O_2 g^{-1} wet mass h^{-1}), mantle contraction frequency (MC min^{-1}), mantle contraction strength (Δ mantle diameter, mm), burst frequency (number of escape jets per min), % relaxed mantle diameter (mm), stroke volume (ml), ventilatory minute volume (ml min^{-1}) and oxygen extraction efficiency (%) with (20%, 50% and 60%) and without potential skin respiration in *Dosidicus gigas*

	d.f.	MS	*F*	*P*
Metabolic rate				
Activity (A)	3	31.5	1.1	0.343
O_2 treatment (T)	2	2804.1	100.9	0.000
A x T	6	125.5	4.5	0.001
Error	60	27.8		
Mantle contraction frequency				
Activity (A)	3	589.6	40.5	0.000
O_2 treatment (T)	2	19,587.0	1343.8	0.000
A x T	6	1809.1	124.1	0.000
Error	60	14.6		
Mantle contraction strength				
Activity (A)	3	3.0	61.3	0.000
O_2 treatment (T)	2	31.5	641.3	0.000
A x T	6	5.3	107.6	0.000
Error	60	0.0		
Escape jet				
Activity (A)	3	436.8	65.5	0.000
O_2 treatment (T)	1	149.6	22.4	0.000
A x T	3	398.9	59.8	0.000
Error	40	6.7		
Relaxed mantle diameter				
Activity (A)	3	21,079.3	9150.8	0.000
O_2 treatment (T)	2	79,802.6	34,643.2	0.000
A x T	6	14,848.1	6445.7	0.000
Error	60	2.3		
Stroke volume				
Activity (A)	3	3.1	27.1	0.000
O_2 treatment (T)	2	72.0	630.9	0.000
A x T	6	11.8	103.0	0.000
Error	60	0.1		
Ventilatory minute volume				
Activity (A)	3	11051.1	66.2	0.000
O_2 treatment (T)	2	288,939.0	1730.4	0.000
A x T	6	46,807.5	280.3	0.000
Error	60	167.0		
O_2 extraction efficiency without potential skin respiration				
Activity (A)	3	3486.7	31.3	0.000
O_2 treatment (T)	2	14149.2	127.2	0.000
A x T	6	3631.4	32.6	0.000
Error	60	111.3		
O_2 extraction efficiency with 20% potential skin respiration				
Activity (A)	3	2276.2	29.5	0.000
O_2 treatment (T)	2	9340.1	120.9	0.000
A x T	6	2403.0	31.1	0.000
Error	60	77.3		
O_2 extraction efficiency with 50% potential skin respiration				
Activity (A)	3	823.5	24.1	0.000
O_2 treatment (T)	2	3751.6	109.6	0.000
A x T	6	878.4	25.7	0.000
Error	60	34.2		
O2 extraction efficiency with 60% potential skin respiration				
Activity (A)	3	527.6	24.1	0.000
O2 treatment (T)	2	2404.1	109.8	0.000
A x T	6	563.0	25.7	0.000
Error	60	21.9		